Author Manuscript

Author Manuscript

Author Manuscript

Author Manuscript

HHS Public Access

Author manuscript

Nanomedicine. Author manuscript; available in PMC 2021 October 01.

Published in final edited form as:

Nanomedicine. 2020 October ; 29: 102236. doi:10.1016/j.nano.2020.102236.

Anti-CD99 scFv-ELP nanoworms for the treatment of acute myeloid leukemia

Vijaya Pooja Vaikari, Ph.D[1,#], **Mincheol Park, B.S**[2,#], **Lena Keossayan, B.S**[1], **J. Andrew MacKay, Ph.D**[2,3,4], **Houda Alachkar, Ph.D**[1,5,*]

[1]Department of Clinical Pharmacy, School of Pharmacy, University of Southern California, Los Angeles, CA 90089, United States

[2]Department of Pharmacology and Pharmaceutical Sciences, School of Pharmacy, University of Southern California, Los Angeles, CA 90089, United States

[3]Department of Ophthalmology, USC Roski Eye Institute, Keck School of Medicine, University of Southern California, Los Angeles, CA 90089, United States

[4]Department of Biomedical Engineering, Viterbi School of Engineering, University of Southern California, Los Angeles, CA 90089, United States

[5]USC Norris Comprehensive Cancer Center, University of Southern California, Los Angeles, CA 90089, United States

Abstract

CD99 is a transmembrane glycoprotein shown to be upregulated in various malignancies. We have previously reported CD99 to be highly upregulated and presents a viable therapeutic target in acute myeloid leukemia (AML). Currently, no therapy against CD99 is under clinical investigation. As a surface molecule, CD99 can be targeted with an antibody-based approach. Here, we have developed a new modality to target CD99 by engineering a fusion protein composed of a single-chain variable fragment antibody (anti-CD99 scFv) conjugated with a high molecular weight elastin-like polypeptide (ELP), A192: α-CD99-A192. This fusion protein assembles into multi-valent nanoworm with optimal physicochemical properties and favorable pharmacokinetic parameters (half-life ~16 hours). α-CD99-A192 nanoworms demonstrated excellent *in vitro* and *in vivo* anti-leukemic effects. α-CD99-A192 induced apoptotic cell death in AML cell lines and primary blasts and prolonged overall survival of AML xenograft mouse model.

Graphical Abstract

*Corresponding Author information: Houda Alachkar, PharmD, Ph. D, Assistant Professor, University of Southern California, School of Pharmacy, 1985 Zonal Avenue John Stauffer Pharmaceutical Sciences Center Room 608, Los Angeles CA 90089, Telephone: 323-442-2696, alachkar@usc.edu.

#both authors contributed equally to the manuscript

Declaration of interest statement

JAM, MP, PV, and HA are inventors on pending provisional patent application related to this work.

Publisher's Disclaimer: This is a PDF file of an unedited manuscript that has been accepted for publication. As a service to our customers we are providing this early version of the manuscript. The manuscript will undergo copyediting, typesetting, and review of the resulting proof before it is published in its final form. Please note that during the production process errors may be discovered which could affect the content, and all legal disclaimers that apply to the journal pertain.

Author Manuscript Author Manuscript Author Manuscript Author Manuscript

The transmembrane protein CD99 is overexpressed in acute myeloid leukemia and presents a viable therapeutic target. We developed a fusion protein composed of anti-CD99 single-chain variable fragment antibody conjugated with an elastin-like polypeptide: α-CD99-A192. This fusion protein assembles into multi-valent nanoworms with an excellent half-life (~16 h). The generated nanoworms bind specifically to cell surface CD99, demonstrate strong anti-leukemic effects *in vitro* and reduce leukemic burden *in vivo.*

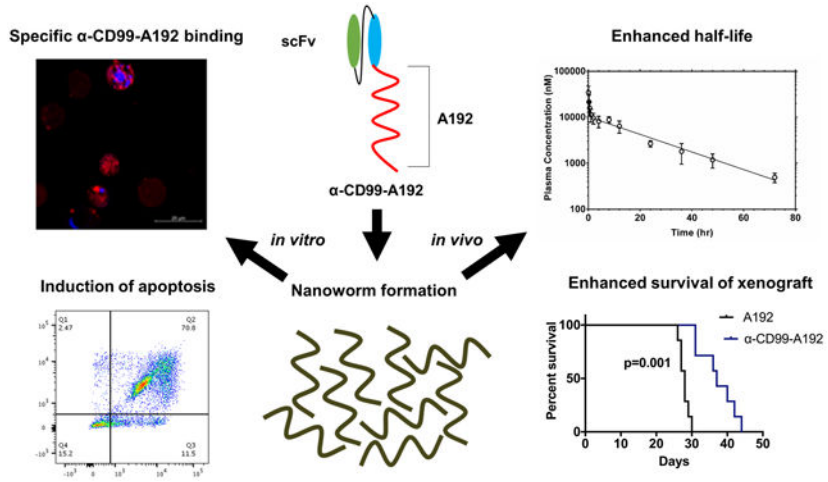

Keywords

CD99; AML; ELP; therapeutic target

Background

Despite recent advances in translating the biology of acute myeloid leukemia (AML) into clinically approved drugs, the majority of patients with AML die of their disease.[1] There hasn't been a breakthrough therapeutic approach that transformed the dismal outcome of AML in decades. We have recently shown that CD99 is highly expressed in AML compared with normal hematopoietic cells.[2] We also established via gain and loss of function approaches that CD99 presents a viable therapeutic target in AML. Silencing CD99 decreased cell proliferation and increased apoptosis. Targeting CD99 with a monoclonal antibody (mAb) resulted in a significant anti-leukemic activity. Anti-CD99mAb drastically reduced cell proliferation and migration of leukemic cells and increased cell apoptosis and differentiation.[2] Anti-CD99mAb was also shown by others to significantly reduce leukemic burden in AML xenograft models and demonstrating *in vivo* anti-leukemia activity.[3]

Monoclonal Antibodies specific to CD99 have been generated by different groups in the past. However, translating mAbs into clinical trials is hampered by cumbersome development process and costs. An alternate solution is the use of single-chain antibody fragments (scFvs). scFvs are about 30 kDa consisting of variable regions of heavy (VH) and light (VL) chains, joined by a flexible peptide linker. scFvs possess specificity equivalent to mAbs and are more readily manipulated using recombinant protein engineering. scFvs can be produced in *Escherichia Coli*[4] compared with the production of mAbs in mammalian

Author Manuscript Author Manuscript Author Manuscript Author Manuscript

systems.[5] A drawback of scFvs, however, is their rapid glomerular filtration in the kidneys, resulting in their short half-life.[6] Challenges involving their purification and low stability also affect their suitability for therapy development.[7] To overcome these limitations, we developed anti-CD99 scFv fused to an elastin-like polypeptide (ELP), A192. ELPs are derived from human tropoelastin and are genetically engineered protein polymers consisting of the amino acid sequence $(VPGXG)_n$. "X" represents a guest amino acid, and "n" indicates the number of the pentameric repeats.[8] As similar sequences are found in human tropoelastin, ELPs are biocompatible and biodegradable. More vitally, ELPs undergo reversible phase separation above a tunable transition temperature that allows them to be purified without chromatography.[9] We previously described that fusion of CD20 scFv to A192 generated a soluble bioactive nanoparticle that assembles into wormshaped nanoparticles with an effective anti-cancer potential in B-cell lymphoma.[10]

Here, we report the development of a new nanoworm that targets CD99, resulting in a strong anti-leukemic activity with an added advantage of optimal colloidal stability and an extended pharmacokinetic half-life as a potential therapy for AML.

Methods

Cloning and purification strategy of α-CD99-A192

To generate an elastin-like polypeptide (ELP) targeting CD99, the α-CD99 scFv gene was fused to the amino terminus of an ELP called A192, in the pET-25b (+) vector, encoding α-CD99-A192. The sequence and cloning method are described in supplementary methods. To produce the fusion protein, Clearcoli® BL21 (DE) Electrocompetent Cells (60810, Lucigen, WI, USA) were transformed with the α-CD99-A192 plasmid using electroporation, and the fusion protein was purified by using three cycles of hot and cold temperature. To maximize the biological activity of α-CD99-A192, the purified protein was urea-denatured and then refolded. The detailed purification and refolding method are described in supplementary methods.

α-CD99-A192 protein concentration measurements

As forming nanoparticles, the fusion protein was denatured with 6 M guanidine hydrochloride to disrupt the assembly of nanoworms. Then, the protein concentration was measured using the following equation:

$$C_{ELP} = \frac{A_{280} - A_{350}}{\varepsilon l} \quad (1)$$

Where A_{280} is the absorbance at 280 nm, A_{350} is the absorbance at 350 nm, ε is the molecular extinction coefficient at 280 nm, and I is the path length (cm). To obtain ε, the following equation was employed[11]:

$$\varepsilon = 125 n_{Cystine} + 5500 n_{Tryptophan} + 1490 n_{Tyrosine} \quad (2)$$

Author Manuscript Author Manuscript Author Manuscript Author Manuscript

Using the above equation, ε of α-CD99 scFv was estimated to be 41,620 L mol^{-1} cm^{-1} assuming all pairs of cysteine residues are oxidized to form cystine, ε of A192 was estimated to be 1,490 L mol^{-1} cm^{-1} as it has only one tyrosine at the end of A192 sequence. Therefore, ε of α-CD99-A192 was estimated to be 43,110 L mol^{-1} cm^{-1}. The optical absorbance at 280 and 350 nm was measured with a NanoDrop 2000 (ThermoFisher Scientific Inc., Waltham, MA, USA), which has a path length of 0.1 cm.

α-CD99-A192 purity and transition temperature analysis

The purity of α-CD99-A192 was determined by an SDS-PAGE gel image quantified using ImageJ. 10 and 20 μg of α-CD99-A192 was loaded to a 4-20% precast SDS-PAGE gel (4561095, Bio-Rad Laboratories, CA, and USA). The gel was stained with Gelcode™ Blue Safe Protein Stain (24596, Thermo Fisher, MA, USA). The gel was imaged with a ChemiDoc Touch Image System (Bio-Rad Laboratories, CA, USA), and analyzed with ImageJ (NIH, MD, USA). A whole lane was plotted to obtain the area under each peak, and the following equation was used to calculate the purity of the protein:

$$\%\ purity = \left(\frac{A_{peak}}{A_{total\ peak}}\right) \times 100\,\% \tag{3}$$

A_{peak} is the area under the peak of the interest, and A_{total} peak is the area under all peaks observed on the SDS-PAGE gel. The transition temperature (T_t) of the fusion protein was measured using Beckman Coulter DU 800 UV/VIS spectrometer (Beckman Coulter, CA, USA). Four different concentrations of α-CD99-A192, 3.125, 6.25, 12.5, and 25 μM were prepared, and the samples were heated at a rate of 1 °C/min. starting from 20 °C to 85 °C. OD_{350} was measured every 18 seconds, and the T_t was determined where the maximum first derivative of the OD_{350} with respect to temperature occurred. The data was fit to the following equation:

$$T_t = b - m log_{10}[C_{ELP}] \tag{4}$$

Where b is the y-intercept representing the extrapolated T_t at a concentration of 1 μM, m is a slope representing the change in °C per 10-fold change in ELP concentration, C_{ELP}.

Measurements of the hydrodynamic radius of α-CD99-A192 and colloidal stability

The hydrodynamic radius and stability of α-CD99-A192 was measured using dynamic light scattering (DLS). To measure the hydrodynamic radius, 25 μM of α-CD99-A192 was prepared, filtered with a 0.22 μm filter, and 60 μl of the protein was added to each well of a 384-well plate. To prevent evaporation of the protein, 15 μl of mineral oil was added. The hydrodynamic radius was measured with DynaPro Plate reader II (Wyatt Technology, CA, USA) at 37 °C. The hydrodynamic radius of A192 was also measured to observe the difference between the fusion protein and A192 in the hydrodynamic radius. The stability of α-CD99-A192 was measured with the same sample. The DLS plate was incubated at 37 °C, and every 24 hours, the hydrodynamic radius of α-CD99-A192 was measured until 72 hours.

Author Manuscript Author Manuscript Author Manuscript Author Manuscript

Measurement of absolute size and weight of α-CD99-A192 nanoworms

The absolute molecular mass of α-CD99-A192 nanoworms was measured with size exclusion chromatography-multi-angle light scattering (SEC-MALS). To run SEC-MALS, 10 μM of α-CD99-A192 was prepared, and the sample was filtered with 0.22 μm filter. A Shodex protein KW-804 (8.0mmI.D.x300mm) (Showa Denko America, NY, USA) was equilibrated with PBS, and the fusion protein was loaded to the column. The fusion protein elusion was observed with three detectors, UV 210 mm detector (SYC-LC-1200) (Agilent Technologies, CA, USA), multi-angle static light scattering detector (DAWN HELEOS) (Wyatt Technology, CA), and differential refractometer (Optilab rEX) (Wyatt Technology). The data were analyzed by ASTRA 6 software.

Patient Samples

Peripheral blood was obtained from a patient with AML at the time of diagnosis at the Norris Comprehensive Cancer Center at USC as well as from healthy donor following written informed consent. The use of human materials was approved by the Institutional Review Boards of USC in accordance with the Helsinki Declaration.

Cell Culture

U937 and MOLM-13 cells were kindly provided by Dr. Wendy Stocks's lab at the University of Chicago. MV4-11 cells were purchased from ATCC. Cell lines were authenticated at the University of Arizona Cell Authentication Core. Cells were cultured in Roswell Park Memorial Institute 1640 (RPMI 1640) medium (Thermo Fisher, MA, USA) supplemented with 10% fetal bovine serum (FBS) and 100 U/mL penicillin (Thermo Fisher). Primary cells (USC001) were grown in RPMI plus FBS (20%) and cytokine cocktails CC100 (Flt3L, SCF, IL-3 and IL-6).

Viability assays

Cell viability was analyzed by trypan blue assay (Life Technologies, Carlsbad, USA) at 72 hours. IC_{50} was determined at 72 hours using alamar blue (Invitrogen, Carlsbad, USA). The detailed method is in supplementary methods.

α-CD99-A192 competitive binding study

Binding of A192 or α-CD99-A192 to cell-surface CD99 was assessed by flow cytometry and Confocal Laser Scanning Microscope (Zeiss, Germany). The detailed method is in supplementary methods.

Flow cytometry analysis

Apoptosis assay was performed using Annexin V-PI kit according to the manufacture's protocol (Invitrogen, Cat no: 88-8007-72). The percentage of apoptotic cells (APC^+ cells) was normalized to untreated cells. For *in vivo* experiments, cell-surface expression of human-CD45 (huCD45: cat.no:25-0459-41, eBioscience, CA, USA) were measured to confirm engraftment. Mouse peripheral blood, bone marrow, and spleen cells were stained with PE-Cy7-A conjugated anti-huCD45. Unbound anti-huCD45 washed away and measured via flow cytometry. MFI of PE-Cy7-A was used to quantify data. Flow cytometry

Author Manuscript Author Manuscript Author Manuscript Author Manuscript

was performed on the LSRII BD Fortessa X20 and processed using FloJo software (BD, Franklin Lakes, NJ, USA).

Pharmacokinetic (PK) and biodistribution study of α-CD99-A192

To assess PK parameters of α-CD99-A192 in mice, 150 μl/20g BW of 340 μM of the NHS-rhodamine-labeled α-CD99-A192 was injected via tail vein into 4 to 6-week-old NOD-*scid* /Il2rg$^{-/-}$ (NSG) female mice (n=4). Blood was collected by venipuncture and mixed with 80 μl of heparinized cold PBS (1,000 U/ml) at: 3 minutes, 15 minutes, 30 minutes, 1 h, 2 h, 4 h, 8 h, 12 h, 24 h, 36 h, 48 h, and 72 h post-injection. Plasma was isolated by centrifugation and diluted plasma was transferred to a 96-well plate, and fluorescence (Excitation/Emission: 540/580 nm) was measured using Synergy H1 Hybrid Multi-Mode Reader (Biotek, VT, USA). Standard curves were generated from the fluorescence measurements of 2, 5, 14, 41, 123, 370, 1111, 3333, and 10000 nM of rhodamine-labeled α-CD99-A192. Following the PK study, kidneys, liver, and spleen were imaged for bioluminescence using the iBright FL1000 gel-imager (Thermofisher). For quantitative analysis, ROIs for fluorescence intensity were analyzed with ImageJ.

In vivo efficacy studies

Animal protocols were approved by the Institution for Animal Care and Use Committee of the University of Southern California. 2.5×10^6 MOLM-13 cells were administered via tail vein injection into 4- to 6-week-old female NOD-*scid* /Il2rg$^{-/-}$ (NSG) mice from Jackson Laboratory (Bar Harbor, ME). Engrafted mice were treated with 200 μL of 220 μM A192 (n=4) or α-CD99-A192 (n=4) via tail vein on Day 7, 10, 13 and 16 post engraftments. Mice were euthanized on Day 21 and spleen, bone marrow and blood were collected and stained for huCD45 and analyzed using flow cytometry. For survival analysis, male mice engrafted with MOLM-13 cells were treated with 200 μL of 220 μM of A192 (n=7) or α-CD99-A192 (n=7) on days 7, 10, 13 and 16 post MOLM-13 engraftment. Mice were euthanized when they displayed signs of severe weight loss, lethargy, hair loss, and/or hunched appearance.

Statistical Analysis

For confocal and bio-distribution image analysis, a global one-way ANOVA followed by the Tukey post-hoc test was used to determine whether mean values are significantly different between groups. The student *t* test was used to determine the significance in means between two groups for viability, apoptosis, and engraftment analysis. Mice survival analysis was performed by the Kaplan Meier survival analysis based on Log-rank (Mantel Cox). For all analyses, $p < 0.05$ was considered significant. All the data is presented as mean ± standard deviation (SD).

Results

Characterization of α-CD99-A192 nanoworms

The fusion protein was purified through induction of temperature-dependent reversible phase separation of A192, and the yield of α-CD99-A192, expressed in Clearcoli® BL21, was calculated to be 34 mg/L with a purity of ~74% (Fig.1B). The purity measured on fluorescent imaging of an SDS-PAGE gel with NHS-rhodamine labeled α-CD99-A192 was

Author Manuscript Author Manuscript Author Manuscript Author Manuscript

~77%. The fusion of α-CD99 scFv to A192 resulted in lower transition temperature (T_t) compared to A192 alone. As shown in Fig. 1C, α-CD99-A192 phase separates above 45.3 °C while A192 phase separates above 59.9 °C (25 μM in PBS). DLS analysis shows that α-CD99-A192 forms nanoworms at 37 °C with a hydrodynamic radius of 46.6 ± 0.5 (mean ± SD, n=6) nm (Fig. 1D). The polydispersity of α-CD99-A192 was measured to be 7.18 ± 0.88 (mean ± SD, n=6) nm, suggesting α-CD99-A192 nanoworms are monodisperse. The hydrodynamic radius of α-CD99-A192 was monitored for 72 hours, which demonstrated that α-CD99-A192 nanoworms are stable colloids at 37 °C (Fig. 1E). The average of absolute mass of nanoworms was analyzed with SEC-MALS and indicated that approximately 170 α-CD99-A192 molecules form a nanoworm (Fig. 1F). The R_g/R_h ratio is equal to 1.0 for the major peak, which is consistent with an elongated spherical shape that resembles nanoworms (Table 1).[12]

α-CD99-A192 binds specifically to CD99 surface protein *in vitro*

The binding affinity of α-CD99-A192 was assessed to confirm the specificity of α-CD99-A192 in $CD99^+$ AML cell lines MOLM-13, MV4-11, U937, and $CD99^-$ 293T cells. Flow cytometry analysis revealed that rhodamine-labeled α-CD99-A192 showed higher binding to MOLM-13 compared with A192 at 1 μM (2.4-fold; p=0.04) and 10 μM (3.1-fold; p=0.01) (Fig. 2A). In MV4-11, a higher level of binding was also observed for α-CD99-A192 compared with A192 at 1 μM (1.7-fold; p=0.001) and 10 μM (2.8-fold; p=0.02) (Fig. 2B). Similarly, in U937 cells, α-CD99-A192 binding was observed at 1 μM (1.5-fold; p=0.002) and 10 μM (1.9-fold; p=0.0001) (Fig. 2C). α-CD99-A192 did not bind to $CD99^-$ 293T suggesting that the binding was specific to CD99 (Fig. 2D). A192 at 1 μM or 10 μM showed no binding to the cells as compared with untreated cells.

To further establish the specificity of α-CD99-A192 binding to CD99, a competitive binding assay was performed. MOLM-13 cells pre-treated with either mAbCD99 or IgG were washed and then treated with rhodamine-labeled α-CD99-A192. After normalizing to untreated cells, cells pretreated with 2.5 and 5 μg/mL mAbCD99 had a significant decrease in binding to α-CD99-A192 as compared to cells treated with α-CD99-A192 alone (~35%, p=0.03 and ~60%, p=0.001 respectively). Pre-treatment with IgG did not affect the binding of α-CD99-A192 to surface CD99. No binding was observed in cells treated with rhodamine-labeled A192 (Fig. 2E). Similarly, confocal microscopy images showed that the treatment of CD99 mAb significantly inhibited the binding of α-CD99-A192 (10 μM) to CD99 surface protein, while IgG did not affect the binding of α-CD99-A192, indicating that the binding of α-CD99-A192 is specific to CD99 (Fig 2F).

α-CD99-A192 induces apoptotic cell death in AML cells

To determine the anti-leukemia activity of α-CD99-A192, MOLM-13, MV4-11 and U937 cells were treated with α-CD99-A192 or A192 at 1, 10, 25 and 50 μM. A significant decrease in the percentage of viable cells was observed in MOLM-13 cells treated with α-CD99-A192 compared with A192 treated cells at 1 μM (p<0.0001, 30% decrease), 10 μM (p<0.0001, 43% decrease), 25 μM (p<0.0001, 78% decrease) and 50 μM (p<0.0001, 82% decrease) (Fig. 3A and S1). In MV4-11 cells, α-CD99-A192 significantly reduced cell viability at 1 μM (p<0.0001, 30% decrease), 10 μM (p<0.0001, 46% decrease), 25 μM

Author Manuscript Author Manuscript Author Manuscript Author Manuscript

(p<0.0001, 80% decrease) and 50 μM (p<0.0001, 84% decrease) (Fig. 3B). Similarly, in U937 cells α-CD99-A192 significantly reduced cell viability at 1 μM (p<0.0001, 30% decrease), 10 μM (p<0.0001, 41% decrease), 25 μM (p<0.0001, 75% decrease) and 50 μM (p<0.0001, 83% decrease) (Fig. 3C). IC_{50} values of α-CD99-A192 for MOLM-13, MV4-11 and U937 cells were determined as 8.1 μM, 4.9 μM and 6.05 μM, respectively (Fig. 3D-F). We also assessed the activity of α-CD99-A192 in healthy donor peripheral blood mononuclear cells (PBMCs) and indeed found that α-CD99-A192 did not exhibit any cytotoxic effect (Fig. S2). This is also consistent with our previous study wherein anti-CD99 monoclonal antibody did not affect the viability of healthy PBMC.[2]

Furthermore, the decrease in cell viability was associated with enhanced apoptosis in α-CD99-A192 treated cells. Annexin V staining revealed a significant increase at 72 hours in MOLM-13 cells treated with α-CD99-A192 (1 μM: p=0.03,1.3-fold; 10 μM: p=0.01, 1.5-fold; 25 μM: p=0.001, 1.6-fold and 50 μM: p=0.01, 1.6-fold; Fig. 4A). In MV4-11 cells treated with α-CD99-A192 showed higher levels of apoptosis compared with A192 treated cells (1 μM: p=0.04,1.4-fold; 10 μM: p=0.005, 1.7-fold; 25 μM: p=0.007, 2-fold and 50 μM: p=0.007, 2-fold; Fig. 4B). Similarly, in U937 cells treated with α-CD99-A192 showed higher levels of apoptosis compared with A192 treated cells (1 μM: p=0.04,1.48-fold; 10 μM: p=0.007, 1.7-fold; 25 μM: p=0.01, 2.3-fold and 50 μM: p=0.009, 2.3-fold; Fig. 4C).

α-CD99-A192 exhibits anti-leukemia activity in primary AML cells

The effect of α-CD99-A192 was further examined in primary AML cells (USC001). Rhodamine-labeled α-CD99-A192 (20 μM) significantly bound to surface CD99 protein compared with A192 (2.6-fold, p<0.001; Fig. 5A). Additionally, α-CD99-A192 significantly reduced cell viability of AML primary cells (24 hours: p=0.002, 50% decrease; 48 hours μM: p<0.0001, 50% decrease; Fig. 5B). This was also accompanied by a significant increase in cell apoptosis at 48 hours (p=0.002, 1.2-fold; Fig. 5C).

PK profile of α-CD99-A192 nanoworms fits the biexponential decay model

PK analysis of α-CD99-A192 indicated that α-CD99-A192 nanoworms fit a biexponential decay model using the following equation:

$$\mathbf{Cp} = \mathbf{A}e^{-\alpha t} + Be^{-\beta t} \quad (5)$$

Where A, B, α, and β are ‘macroconstants’ that can be fit with nonlinear regression. Using both non-compartmental and two-compartmental analysis, the PK parameters of α-CD99-A192 were obtained (Table 2). The terminal half-life of the fusion protein was 15.8 hours, and mean residence time was 21.3 hours (Fig. 6A). These pharmacokinetic findings justify treatment intervals up to 3-5 days. The clearance of the fusion protein was determined to be 0.28 mL/hr, which is consistent with other reported clearance of high molecular weight ELPs.[13, 14] The volume of distribution was calculated to be 1.92 mL, which is consistent with the expected volume of blood in these mice. Bioluminescence images of spleen, kidneys, and liver showed that α-CD99-A192 nanoworms still resided in those organs 96 hours post-injection and accumulated at a higher level in the liver as compared to the spleen

Author Manuscript Author Manuscript Author Manuscript Author Manuscript

and kidney ($p \leq 0.05$) (Representative bioluminescence images and quantification Fig. 6B, C and S3 respectively).

α-CD99-A192 reduces leukemia burden and prolongs survival of mice in an AML xenograft model

To determine the therapeutic potential of α-CD99-A192, MOLM-13 cells were administered into NSG mice and treated with α-CD99-A192 or A192 on day 7, 10, 13 and 16 post-leukemia engraftment. Mice in the treatment group had smaller spleens that weighed significantly less compared with the control group (113 *vs.* 180 mg, $p<0.001$) (Fig. 7A). huCD45 analysis revealed that treatment with α-CD99-A192 had significantly less leukemia engraftment compared with the A192 mice in the bone marrow (%huCD45: 29 *vs.* 53%, $p<0.0001$; Fig. 7C-D), peripheral blood (%huCD45: 6 *vs.* 22%, $p<0.001$; Fig.7 E-F) and the spleen (%huCD45: 5 *vs.* 13%, $p<0.0001$; Fig. 7G-H).

The therapeutic effect of α-CD99-A192 was further confirmed in MOLM-13 xenograft model via survival analysis. Mice treated with α-CD99-A192 survived significantly longer than mice in the A192 group (median survival: 37 *vs.* 28 Days, $p<0.0001$; Fig. 7I).

Discussion

CD99 is upregulated in various cancers like Ewing sarcoma, T-lineage acute lymphoblastic leukemia, gliomas and AML.[2, 3, 15-19] As a cell surface molecule, CD99 presents as a viable target for antibody-based therapies. Indeed, the antitumor activity of targeting CD99 with monoclonal antibodies was demonstrated in several preclinical cancer models. In these studies, the use of an antibody against CD99 has resulted in inhibition of cell migration and activation of cell apoptosis.[20-22] In Ewing sarcoma, CD99 mAb resulted in homotypic cell aggregation and caspase-independent cell death. CD99mAb also potentiated the antitumor activity of doxorubicin and vincristine in preclinical studies in Ewing sarcoma and was effective against chemo-resistant tumor cells.[23, 24] CD99 also serves as a diagnostic marker in Ewing Sarcoma.[25] With the extensive evidence backing CD99 mAb high potential in the clinical setting, no antibody against CD99 has yet made it into a clinical investigation as a therapeutic approach. Challenges in antibody development including limitations related to their ineffective clustering on target receptors as well as lack of therapeutic concentrations on target cells hinder monoclonal antibodies from transitioning into clinical development. Our study presents the development and efficacy testing of a new antibody-based CD99 nanoparticle, which is composed of α-CD99 single-chain variable fragment (scFv) linked to A192, an elastin-like polypeptide (ELP), derived from human tropoelastin.

The advantage of fusing A192 to α-CD99 scFv is the resultant high yield of the fusion protein (34 mg/L) in the soluble fraction after bacterial lysis. Because ELPs phase separate above a tunable transition temperature, a chromatography-free, a high purity fusion protein can be obtained without the need for additional purification tags which may hinder protein activity.[26, 27] Using this technique, we were able to achieve high purity of α-CD99-A192 with minimal purification steps (77 % purity by Rhodamine-labeling). Another challenge in developing scFv as therapeutic antibodies is associated with the low stability of scFv fragments.[28-30] Notably, the fusion of A192 to α-CD99 scFv increased its molecular weight,

Author Manuscript Author Manuscript Author Manuscript Author Manuscript

formed nanoworms, and proved to be stable colloids for three days at 37 °C. Although R_g/R_h ratio describes whether macromolecules have a spherical or rod-like structure; to determine the exact shape and particle sizes of α-CD99-A192 nanoworms in their native environment, cryogenic electron microscopy should be employed. PK analysis revealed that the terminal half-life of α-CD99-A192 was 15.8 hours and the MRT was 21.3 hours, which are excellent values compared with free scFvs. These enhanced PK parameters of α-CD99-A192 are attributed to the evasion of glomerular filtration. The cut-off diameter of glomerular filtration for most proteins and metal nanoparticles is close to 10 nm,[31, 32] suggesting that monodisperse α-CD99-A192 nanoworms cannot filter through the glomerulus. A similar effect on pharmacokinetics was reported for an anti-tumor necrosis factor single-chain V_H antibody fused to a soluble ELP.[33] Data extracted from that report (Fig. S4) was analyzed to determine equivalent PK parameters (Table S1), which revealed that the 16.8 kDa single-chain antibody alone had a clearance of 1.3 mL/hr, while its 57.1 kDa fusion to an ELP yielded a clearance of 0.12 mL/hr. The MRT for that single-chain antibody ELP fusion was 17.7 hrs, which falls into the 95% confidence interval for α-CD99-A192 (Table 2). This evidence shows that ELP fusion appears to be a plausible strategy to extend the MRT for single-chain antibodies. We speculate that the long half-life of α-CD99-A192 may be an advantage that makes the fusion protein suitable for further clinical development. In addition, it has been discovered that scFv-ELP phase separation clustered target receptors on the cell membrane after binding and enhanced the internalization of the receptors, resulting in improved biological activity compared to a commercial monoclonal antibody.[10] It is unknown whether CD99 transmembrane glycoproteins get internalized upon binding, but if CD99 shows a similar mechanism to that of receptor proteins that get internalized, we might expect an enhanced therapeutic effect of α-CD99-A192 nanoworms.

Across various AML cell lines, α-CD99-A192 showed positive binding to $CD99^+$ cells but not $CD99^-$ 293T cells. The specificity of the binding was also demonstrated in a competitive-binding assay in MOLM-13 cells. Furthermore, α-CD99-A192 significantly reduced cell viability and increase cell apoptosis in both AML cell lines and primary AML cells. In the MOLM-13 xenograft model, treatment with α-CD99-A192 reduced leukemia burden and significantly improved survival of the mice. Altogether the *In vitro* and *in vivo* testing of α-CD99-A192 established a strong activity of this compound in preclinical models.

In conclusion, this study reports the development and preclinical evaluation of a new therapeutic scFv nanoworm directed against CD99. The fusion of ELP to α-CD99 scFv solubilizes the scFv, facilitates purification of the protein, stabilizes biologically active nanoworms, and enhances PK profiles of α-CD99 scFv. With CD99 serving a therapeutic target for various malignancies, our study suggests α-CD99 scFv-ELP fusion protein can be a candidate therapeutic agent for AML. α-CD99-A192 also has further scope in the clinical setting than evaluated here. Apart from AML, we also speculate that this new scFv against CD99 can be used in several other disease models, such as Ewing sarcoma and gliomas.

Supplementary Material

Refer to Web version on PubMed Central for supplementary material.

Author Manuscript Author Manuscript Author Manuscript Author Manuscript

Acknowledgements

This work was made possible by University of Southern California (USC), the Gavin S. Herbert Professorship, the National Institutes of Health R01 GM114839 to JM, the USC Ming Hsieh Institute, P30 CA014089 to the USC Norris Comprehensive Cancer Center, P30 EY029220 to the USC Ophthalmology Center Core Grant for Vision Research, Center of Excellence in Nanobiophysics at USC, and the Translational Research Laboratory at USC School of Pharmacy.

References

1. Dohner H, Estey E, Grimwade D, Amadori S, Appelbaum FR, Buchner T, et al. Diagnosis and management of AML in adults: 2017 ELN recommendations from an international expert panel. Blood. 2017;129:424–47. [PubMed: 27895058]
2. Vaikari VP, Du Y, Wu S, Zhang T, Metzeler K, Batcha AMN, et al. Clinical and preclinical characterization of CD99 isoforms in acute myeloid leukemia. Haematologica. 2019.
3. Chung SS, Eng WS, Hu W, Khalaj M, Garrett-Bakelman FE, Tavakkoli M, et al. CD99 is a therapeutic target on disease stem cells in myeloid malignancies. Sci Transl Med. 2017;9.
4. Skerra A, Pluckthun A. Assembly of a functional immunoglobulin Fv fragment in Escherichia coli. Science. 1988;240:1038–41. [PubMed: 3285470]
5. Hu X, O'Hara L, White S, Magner E, Kane M, Wall JG. Optimisation of production of a domoic acid-binding scFv antibody fragment in Escherichia coli using molecular chaperones and functional immobilisation on a mesoporous silicate support. Protein Expres Purif. 2007;52:194–201.
6. Hutt M, Farber-Schwarz A, Unverdorben F, Richter F, Kontermann RE. Plasma half-life extension of small recombinant antibodies by fusion to immunoglobulin-binding domains. J Biol Chem. 2012;287:4462–9. [PubMed: 22147690]
7. Hayhurst A, Harris WJ. Escherichia coli skp chaperone coexpression improves solubility and phage display of single-chain antibody fragments. Protein Expr Purif. 1999;15:336–43. [PubMed: 10092493]
8. Despanie J, Dhandhukia JP, Hamm-Alvarez SF, MacKay JA. Elastin-like polypeptides: Therapeutic applications for an emerging class of nanomedicines. J Control Release. 2016;240:93–108. [PubMed: 26578439]
9. Christensen T, Amiram M, Dagher S, Trabbic-Carlson K, Shamji MF, Setton LA, et al. Fusion order controls expression level and activity of elastin-like polypeptide fusion proteins. Protein science : a publication of the Protein Society. 2009;18:1377–87. [PubMed: 19533768]
10. Aluri SR, Shi P, Gustafson JA, Wang W, Lin YA, Cui H, et al. A hybrid protein-polymer nanoworm potentiates apoptosis better than a monoclonal antibody. ACS Nano. 2014;8:2064–76. [PubMed: 24484356]
11. Pace CN, Vajdos F, Fee L, Grimsley G, Gray T. How to Measure and Predict the Molar Absorption-Coefficient of a Protein. Protein Science. 1995;4:2411–23. [PubMed: 8563639]
12. Nygaard M, Kragelund BB, Papaleo E, Lindorff-Larsen K. An Efficient Method for Estimating the Hydrodynamic Radius of Disordered Protein Conformations. Biophys J. 2017;113:550–7. [PubMed: 28793210]
13. Lee C, Guo H, Klinngam W, Janga SR, Yarber F, Peddi S, et al. Berunda Polypeptides: Biheaded Rapamycin Carriers for Subcutaneous Treatment of Autoimmune Dry Eye Disease. Mol Pharm. 2019;16:3024–39. [PubMed: 31095909]
14. Guo H, Lee C, Shah M, Janga SR, Edman MC, Klinngam W, et al. A novel elastin-like polypeptide drug carrier for cyclosporine A improves tear flow in a mouse model of Sjogren's syndrome. J Control Release. 2018;292:183–95. [PubMed: 30359668]
15. Choi YL, Chi JG, Suh YL. CD99 immunoreactivity in ependymoma. Appl Immunohistochem Mol Morphol. 2001;9:125–9. [PubMed: 11396629]
16. Ambros IM, Ambros PF, Strehl S, Kovar H, Gadner H, Salzer-Kuntschik M. MIC2 is a specific marker for Ewing's sarcoma and peripheral primitive neuroectodermal tumors. Evidence for a common histogenesis of Ewing's sarcoma and peripheral primitive neuroectodermal tumors from MIC2 expression and specific chromosome aberration. Cancer. 1991;67:1886–93. [PubMed: 1848471]

Author Manuscript Author Manuscript Author Manuscript Author Manuscript

17. Buxton D, Bacchi CE, Gualco G, Weiss LM, Zuppan CW, Rowsell EH, et al. Frequent expression of CD99 in anaplastic large cell lymphoma: a clinicopathologic and immunohistochemical study of 160 cases. Am J Clin Pathol. 2009;131:574–9. [PubMed: 19289593]
18. Kavalar R, Pohar Marinsek Z, Jereb B, Cagran B, Golouh R. Prognostic value of immunohistochemistry in the Ewing's sarcoma family of tumors. Med Sci Monit. 2009;15:Cr442–52. [PubMed: 19644423]
19. Zhang PJ, Barcos M, Stewart CC, Block AW, Sait S, Brooks JJ. Immunoreactivity of MIC2 (CD99) in acute myelogenous leukemia and related diseases. Mod Pathol. 2000; 13:452–8. [PubMed: 10786814]
20. Seol HJ, Chang JH, Yamamoto J, Romagnuolo R, Suh Y, Weeks A, et al. Overexpression of CD99 Increases the Migration and Invasiveness of Human Malignant Glioma Cells. Genes Cancer. 2012;3:535–49. [PubMed: 23486730]
21. Cerisano V, Aalto Y, Perdichizzi S, Bernard G, Manara MC, Benini S, et al. Molecular mechanisms of CD99-induced caspase-independent cell death and cell-cell adhesion in Ewing's sarcoma cells: actin and zyxin as key intracellular mediators. Oncogene. 2004;23:5664–74. [PubMed: 15184883]
22. Sohn HW, Choi EY, Kim SH, Lee IS, Chung DH, Sung UA, et al. Engagement of CD99 induces apoptosis through a calcineurin-independent pathway in Ewing's sarcoma cells. Am J Pathol. 1998;153:1937–45. [PubMed: 9846983]
23. Scotlandi K, Baldini N, Cerisano V, Manara MC, Benini S, Serra M, et al. CD99 engagement: an effective therapeutic strategy for Ewing tumors. Cancer Res. 2000;60:5134–42. [PubMed: 11016640]
24. Manara MC, Terracciano M, Mancarella C, Sciandra M, Guerzoni C, Pasello M, et al. CD99 triggering induces methuosis of Ewing sarcoma cells through IGF-1R/RAS/Rac1 signaling. Oncotarget. 2016;7:79925–42. [PubMed: 27835596]
25. Louati S, Senhaji N, Chbani L, Bennis S. EWSR1 Rearrangement and CD99 Expression as Diagnostic Biomarkers for Ewing/PNET Sarcomas in a Moroccan Population. Dis Markers. 2018;2018.
26. Sabaty M, Grosse S, Adryanczyk G, Boiry S, Biaso F, Arnoux P, et al. Detrimental effect of the 6 His C-terminal tag on YedY enzymatic activity and influence of the TAT signal sequence on YedY synthesis. BMC Biochem. 2013; 14:28. [PubMed: 24180491]
27. Goel A, Colcher D, Koo JS, Booth BJ, Pavlinkova G, Batra SK. Relative position of the hexahistidine tag effects binding properties of a tumor-associated single-chain Fv construct. Biochim Biophys Acta. 2000; 1523:13–20. [PubMed: 11099853]
28. Worn A, Pluckthun A. Different equilibrium stability behavior of ScFv fragments: identification, classification, and improvement by protein engineering. Biochemistry. 1999;38:8739–50. [PubMed: 10393549]
29. Brockmann EC, Cooper M, Stromsten N, Vehniainen M, Saviranta P. Selecting for antibody scFv fragments with improved stability using phage display with denaturation under reducing conditions. Journal of Immunological Methods. 2005;296:159–70. [PubMed: 15680160]
30. Worn A, Pluckthun A. Stability engineering of antibody single-chain Fv fragments. J Mol Biol. 2001;305:989–1010. [PubMed: 11162109]
31. Du BJ, Yu MX, Zheng J. Transport and interactions of nanoparticles in the kidneys. Nature Reviews Materials. 2018;3:358–74.
32. Sadauskas E, Wallin H, Stoltenberg M, Vogel U, Doering P, Larsen A, et al. Kupffer cells are central in the removal of nanoparticles from the organism. Part Fibre Toxicol. 2007;4:10. [PubMed: 17949501]
33. Conrad U, Plagmann I, Malchow S, Sack M, Floss DM, Kruglov AA, et al. ELPylated anti-human TNF therapeutic single-domain antibodies for prevention of lethal septic shock. Plant Biotechnol J. 2011;9:22–31. [PubMed: 20444206]
34. Guo H, MacKay JA. A pharmacokinetics primer for preclinical nanomedicine research Nanoparticles for Biomedical Applications: Elsevier; 2020 p. 109–28.

Author Manuscript Author Manuscript Author Manuscript Author Manuscript

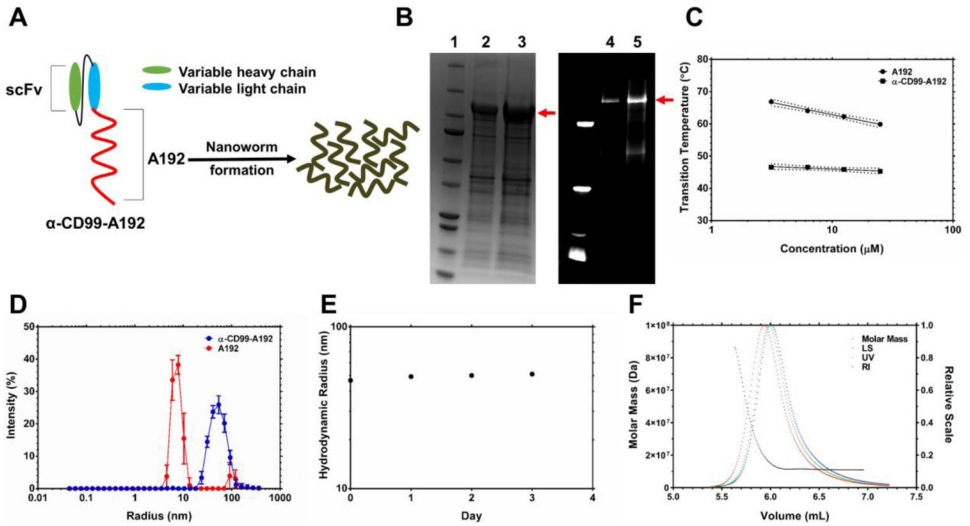

Figure 1. Construction, purification and refolding of a recombinant elastin-like polypeptide (ELP) fusion protein targeting CD99 receptors.

A) To construct an ELP fusion protein targeting CD99 receptors, α-CD99 scFv was fused to the N-terminus of a high molecular weight ELP, A192. It has been frequently observed that scFv-ELP fusion proteins form nanoworms spontaneously in PBS. **B)** The ELP fusion protein was purified by using ELP-mediated temperature-dependent phase separation. Three rounds of hot and cold temperature were used to purify α-CD99-A192, and the purity of the fusion protein was calculated to be 73.5 % based on the analysis of the SDS-PAGE gel on the left side: lane 1: ladder lane 2: 10 μg of α-CD99-A192 lane 3: 20 μg of α-CD99-A192. The SDS-PAGE gel on the right side shows the purity of NHS-rhodamine labeled α-CD99-A192, and the purity was calculated to be 77 %: lane 4: 8.5 μg of NHS-rhodamine labeled α-CD99-A192 lane 5: 17 μg of NHS-rhodamine labeled α-CD99-A192 **C)** The transition temperature of A192 and α-CD99-A192 was measured at 3.125, 6.25, 12.5, and 25 μM. The fusion of α-CD99 scFv to A192 substantially lowers the transition temperature of A192, and the transition temperature is less affected by the change of the protein's concentration. Transition temperature becomes less sensitive to the change of the protein's concentration. **D)** Hydrodynamic radius (R_h) of refolded α-CD99-A192 was measured with DLS at 37 °C. While A192 is monomeric, α-CD99-A192 formed nanoworms. **E)** The stability of α-CD99-A192 in PBS was observed with DLS for 72 hours. The R_h of the fusion protein did not change much over 72 hours, indicating that the fusion protein remains stable colloids in PBS at 37 °C. **F)** To measure the absolute molar mass of α-CD99-A192 nanoworms, SEC-MALS was employed. The average molecular weight of a nanoworm was measured to be 1.7×10^7 Da, which is equivalent to the molecular weight of 171 α-CD99-A192 molecules.

Author Manuscript Author Manuscript Author Manuscript Author Manuscript

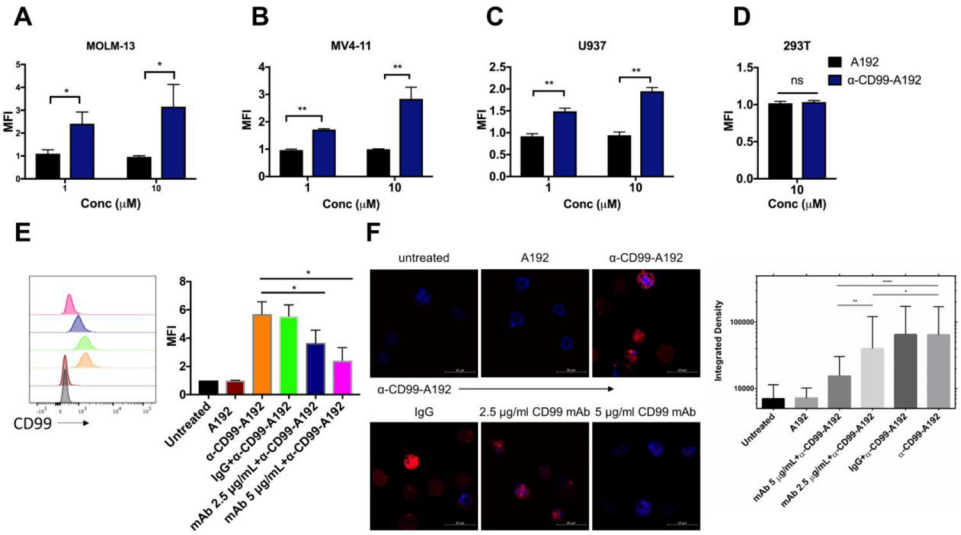

Figure 2. Recombinant α-CD99-A192 binds specifically to CD99.

$CD99^+$ AML cell lines MOLM-13, MV4-11, U937 cells, and $CD99^-$ 293T cells (0.5 x 10^6cellls) were treated with 1 μM or 10 μM of rhodamine labeled α-CD99-A192 or rhodamine-labeled A192 for 30 minutes on ice. The binding was measured via flow cytometry by analyzing the MFI of rhodamine and normalizing data to untreated cells. The significant binding was observed in **A)** MOLM-13 **B)** MV4-11 **C)** U937 cells. **D)** No binding was observed in 293T cells. The competitive binding assay was performed in MOLM-13 cells by pre-treating cells with either CD99 Mab (2.5 μg/mL or 5 μg/mL) or IgG and then observing binding with rhodamine α-CD99-A192 (10 μM). The binding was measured via **E)** Flow cytometry by measuring the peak shift in rhodamine to bound cell and quantifying based on mean fluorescence intensity and **F)** laser scanning confocal microscopy where cell fluorescence was quantified with ImageJ. Data represented as mean ± SD. * p≤0.05 ** p≤0.01*** p≤0.001**** p≤0.0001

Author Manuscript Author Manuscript Author Manuscript Author Manuscript

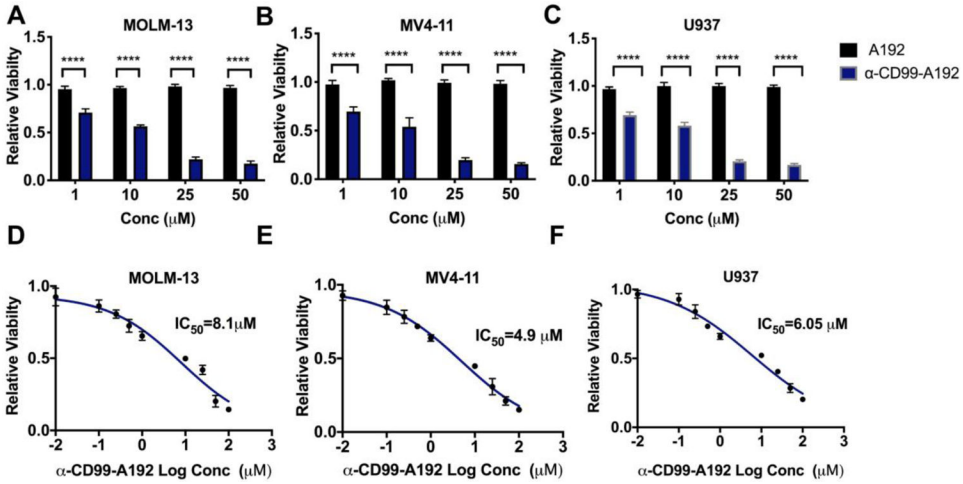

Figure 3: α-CD99-A192 has anti-leukemic activity in AML cells.

A-C) A trypan blue viability assay was performed in MOLM-13, MV4-11, and U937 cells treated with α-CD99-A192 or an A192 control for 72 hours. The number of live cells was normalized to untreated cells. Data represented as mean ± SD, n=6. **D-E)** Alamar blue staining was performed in MOLM-13, MV4-11 and U937 cells to determine the IC_{50} of α-CD99-A192 at 48 hours post-treatment with the increasing concentration of α-CD99-A192 and plotted based on non-linear regression.

Author Manuscript Author Manuscript Author Manuscript Author Manuscript

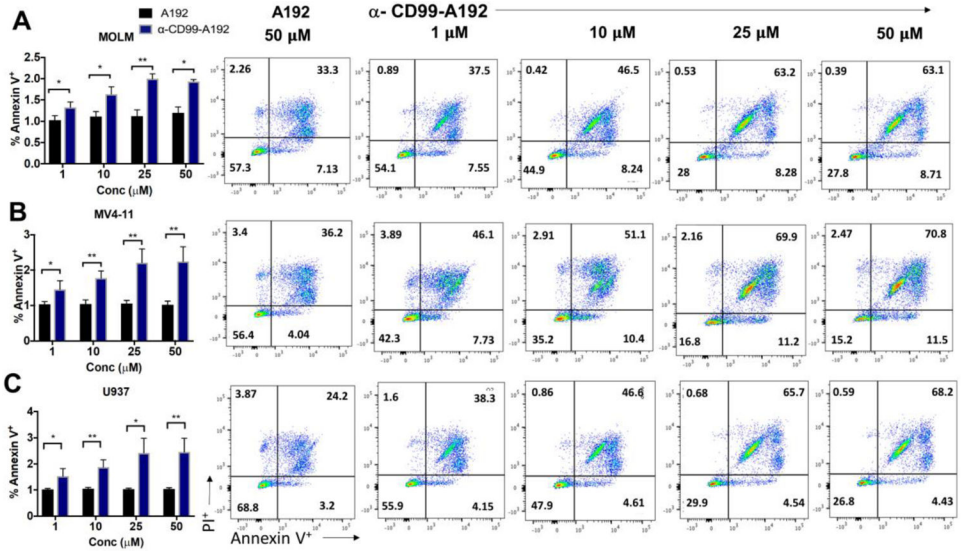

Figure 4: α-CD99-A192 induces apoptosis in AML cells.

Annexin V-PI assay was performed in A) MOLM-13, B) MV4-11 and C) U937 cells treated with α-CD99-A192 or control A192. Apoptosis was measured by flow cytometry using APC conjugated Annexin V stain normalized to untreated cells. Representative flow cytometry images and quantified Annexin V data are presented. Data represented as mean ± SD, n=3.

Author Manuscript Author Manuscript Author Manuscript Author Manuscript

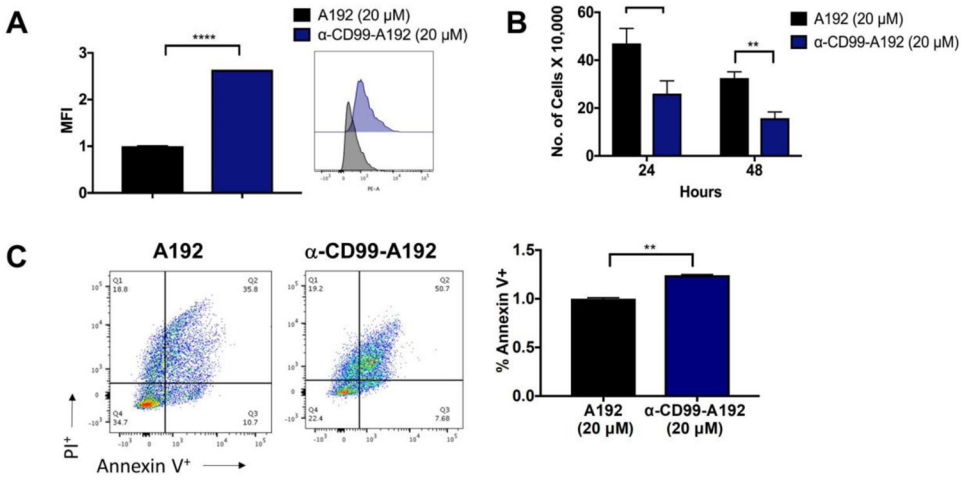

Figure 5: α-CD99-A192 has anti-leukemic activity in primary AML cells.

A) A trypan blue viability assay was performed in MOLM-13, MV4-11 and U937 cells treated with α-CD99-A192 or an A192 control for 72 hours. The number of live cells was normalized to untreated cells. Data represented as mean ± SD, n=6. **B-C)** Alamar blue staining was performed in MOLM-13, MV4-11, and U937 cells to determine the IC_{50} of α-CD99-A192 at 48 hours post-treatment with the increasing concentration of α-CD99-A192 and plotted based on non-linear regression.

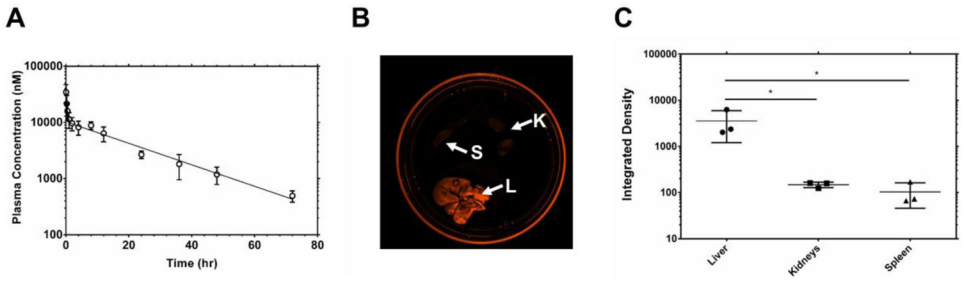

Figure 6. PK profile of α-CD99-A192 nanoworms:

190 μM of α-CD99-A192 labeled covalently with rhodamine in 150 μl/25g B.W. of PBS was injected via tail vein in mice (n=4 mice). Blood was collected and plasma was measured for fluorescence. Rhodamine-labeled α-CD99-A192 plasma concentration was calculated using a standard curve. **A)** The plasma concentrations were fit to **Eq. (6)** to obtain the PK curve, and the generated curve shows the rhodamine-labeled α-CD99-A192 concentration in the plasma over 72 hours. After 96 hours from the injection, spleen (S), kidneys (K), and the liver (L) were collected from mice. **B-C)** Bioluminescence images of organs were obtained 96 hours post-injection and quantified based on the fluorescent intensity obtained from images.

Author Manuscript Author Manuscript Author Manuscript Author Manuscript

Author Manuscript Author Manuscript Author Manuscript Author Manuscript

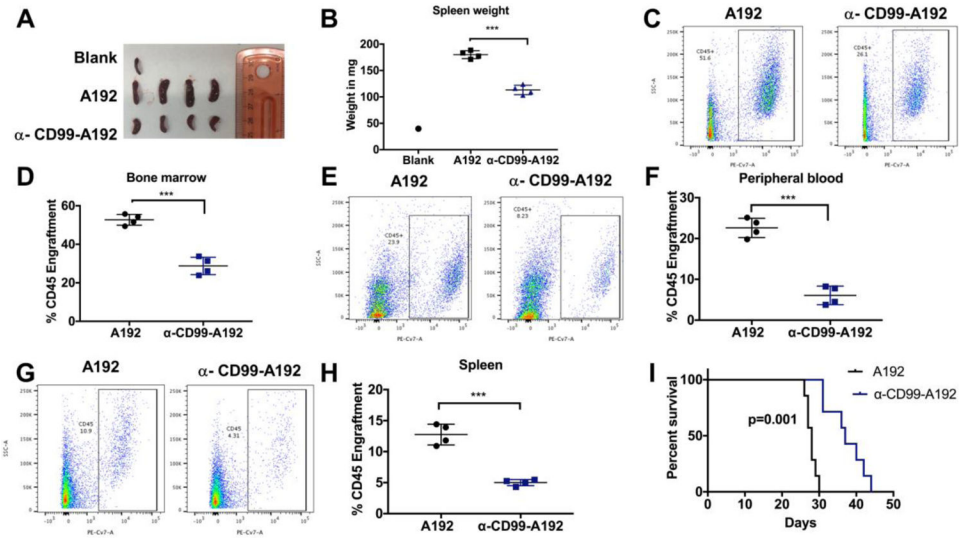

Figure 7: Anti-leukemia activity of α-CD99-A192 in MOLM-13 murine model.

Fig A-H: 2.5×10^6 cells MOLM-13 cells/mouse were engrafted in NSG mice. Mice were treated with 200 μL of 220 μM of A192 (n=4) or α-CD99-A192 (n=4) on day 7, 10, 13 and 16 post engraftment and euthanized on day 17. **A)** Spleen images and **B)** Spleens weights were measured upon euthanization. Spleens of mice treated with α-CD99-A192 weighed significantly less compared with the A192 treated mice (113 *vs.* 180 mg, p<0.001). Leukemia engraftment was measured using human CD45 (huCD45) antibody by flow cytometry in the **C-D**) peripheral blood (%huCD45: 6 *vs.* 22%, p<0.001), **E-F**) bone marrow (29 *vs.* 53%, p<0.0001) and G-H) spleen (%huCD45: 5 *vs.* 13%, p<.0001). **I)** 2.5×10^6 MOLM-13 cells/mouse were engrafted in NSG mice and treated with 200 μL of 220 μM A192 (n=7) or α-CD99-A192 on Day 7, 10, 13 and 16 post engraftment and survival was recorded. Kaplan Meier survival analysis showed that mice in the α-CD99-A192 treatment group survived significantly longer than mice in the A192 group (median survival: 37 *vs.* 28 Days, p<0.0001).

Author Manuscript

Author Manuscript

Author Manuscript

Author Manuscript

Table 1.

Characterization of α-CD99-A192 nanoworms

ELP	Amino acid sequence	M.W. (kDa)[b]	T_t (°C)[c]	R_h (nm)	R_g/R_h	Shape[e]
A192	$G(VPGAG)_{192}Y$	73.6	59.9	7.5 ± 0.2	N/A	monomer
α-CD99-A192	αCD99[a]-$G(VPGAG)_{192}Y$	99.2	45.3	46.6 ± 0.5	1.0[d]	Extended rod-like shape

[a] αCD99 amino acid sequence:

MAEVQLVESGGGLVRPGGSLRLSCAASGFTFSSYAMSWVRQAPGKGLEWVSAISGSGGSTY
YADSVKGRFTISRDNSKNTLYLQMNSLRAEDTAVYYCAKSHKRFDYWGQGTLVTVSRGGGGS
GGGGSGGGGSSELTQDPAVSVALGQTVRITCQGDSLRSYYASWYQQKPGQAPVLVIYGKNN
RPSGIPDRFSGSSSGNTASLTITGAQAEDEADYYCNSSFPRTSSVVFGGGTKLTVLGLVPRGS

[b] It is the expected molecular weight based on the amino acid sequence

[c] Transition temperature was determined at the maximum first derivative of the optical density at 350 nm

[d] This number represents R_g/R_h of peak 1 observed in SEC-MALS

[e] The shape of α-CD99-A192 was determined by using the ratio R_g/R_h, which were obtained from DLS and SEC-MALS

Author Manuscript

Author Manuscript

Author Manuscript

Table 2:

PK parameters for α-CD99-A192

Parameter (Unit)	α-CD99-A192 IV (SD) (n=4)	95% Conf Interval [Lower to Upper bound]
Dose **(nmol)**[a]	66.8 (2.8)	[62.4 to 71.2]
CL **(ml/hr)**[a]	0.28 (0.02)	[0.24 to 0.32]
AUC **(μM*hr)**[a]	240 (17)	[212 to 268]
AUMC **(μM*hr^2)**[a]	5130 (959)	[3610 to 6660]
MRT **(hr)**[a]	21.3 (2.6)	[17.1 to 25.4]
V_{ss} **(mL)**[a]	5.92 (0.63)	[4.91 to 6.92]
C_0 **(μM)**[b]	42.6 (26.3)	[0.8 to 84.5]
A **(μM)**[b]	32.5 (25.2)	[0 to 72.5]
B **(μM)**[b]	10.2 (1.2)	[8.3 to 12.0]
α **(hr^{-1})**[b]	6.13 (5.88)	[0 to 15.5]
β **(hr^{-1})**[b]	0.044 (0.004)	[0.037 to 0.051]
$t_{1/2\alpha}$ **(hr)**[b]	0.24 (0.20)	[0 to 0.56]
$t_{1/2\beta}$ **(hr)**[b]	15.8 (1.4)	[13.5 to 18.1]
$k_{elimination}$ **(hr^{-1})**[b]	0.17 (0.08)	[0.04 to 0.30]
$k_{plasma \rightarrow tissue}$ **(hr^{-1})**[b]	4.61 (5.09)	[0 to 12.7]
$k_{tissue \rightarrow plasma}$ **(hr^{-1})**[b]	1.39 (0.90)	[0 to 2.82]
AUC **(μmol*h)**[b]	239 (36)	[182 to 296]
CL **(ml/h)**[b]	0.28 (0.04)	[0.22 to 0.35]
$V_d{}^{\alpha}$ **(ml)**[b]	1.92 (0.77)	[0.69 to 3.15]

[a]determined using non-compartmental analysis

[b]determined by fitting to Eq. 5 and fit to a two-compartment model of an intravenous bolus[34]